The evolving radio jet from the neutron star X-ray binary 4U 1820−30

T. D. Russell [1,2]★ N. Degenaar [2] J. van den Eijnden [3] M. Del Santo [1] A. Segreto,[1] D. Altamirano,[4] A. Beri [4,5] M. Díaz Trigo[6] and J. C. A. Miller-Jones [7]

[1]*INAF, Istituto di Astrofisica Spaziale e Fisica Cosmica, Via U. La Malfa 153, I-90146 Palermo, Italy*
[2]*Anton Pannekoek Institute for Astronomy, University of Amsterdam, Science Park 904, NL-1098 XH Amsterdam, the Netherlands*
[3]*Astrophysics, Department of Physics, University of Oxford, Denys Wilkinson Building, Keble Road, Oxford OX1 3RH, UK*
[4]*School of Physics and Astronomy, University of Southampton, Highfield SO17 IBJ, UK*
[5]*Department of Physics, Indian Institute of Science Education and Research, Mohali, 140306, India*
[6]*ESO, Karl-Schwarzschild-Strasse 2, D-85748 Garching bei München, Germany*
[7]*International Centre for Radio Astronomy Research, Curtin University, GPO Box U1987, Perth, WA 6845, Australia*

ABSTRACT

The persistently bright ultracompact neutron star low-mass X-ray binary 4U 1820−30 displays an ∼170 d accretion cycle, evolving between phases of high and low X-ray modes, where the 3–10 keV X-ray flux changes by a factor of up to ≈8. The source is generally in a soft X-ray spectral state, but may transition to a harder state in the low X-ray mode. Here, we present new and archival radio observations of 4U 1820−30 during its high and low X-ray modes. For radio observations taken within a low mode, we observed a flat radio spectrum consistent with 4U 1820−30 launching a compact radio jet. However, during the high X-ray modes the compact jet was quenched and the radio spectrum was steep, consistent with optically thin synchrotron emission. The jet emission appeared to transition at an X-ray luminosity of $L_{X(3-10\,keV)} \sim 3.5 \times 10^{37}(D/7.6\,kpc)^2\,erg\,s^{-1}$. We also find that the low-state radio spectrum appeared consistent regardless of X-ray hardness, implying a connection between jet quenching and mass accretion rate in 4U 1820−30, possibly related to the properties of the inner accretion disc or boundary layer.

Key words: accretion, accretion discs – stars: neutron – radio continuum: transients – X-rays: binaries.

1 INTRODUCTION

There is an observed phenomenological relationship between jet production and the accretion process in all accreting compact objects; however, at present the exact nature of the coupling remains to be determined. Neutron star (NS) and black hole (BH) low-mass X-ray binary (LMXB) systems act as useful observational laboratories to study this coupling as they allow for the properties of the in-flowing accretion flow and out-flowing jets to be observed on human time-scales. Changes in the accretion flow are typically observed in the X-rays, while corresponding changes in the jet emission are generally seen in the radio band. In particular, NS LMXBs offer an important observational tool, allowing for the role that stellar surface, spin, and magnetic field play on jet production to be tested. However, due to the relative radio faintness of NS LMXBs (e.g. Gallo, Degenaar & van den Eijnden 2018), our understanding of jet launching in NS LMXBs is generally less evolved than their BH counterparts (e.g. Migliari & Fender 2006).

Jets from accreting NS LMXBs show a diverse range of behaviour (e.g. Migliari & Fender 2006; Migliari 2011; Gusinskaia et al. 2017, 2020; Tudor et al. 2017; Gallo et al. 2018; Russell et al.

2018), and there has been some debate as to whether NS LMXB jets show a similar pattern of behaviour to BH systems (see e.g. Migliari & Fender 2006; Marino et al. 2020). NS and BH LMXBs can launch two types of jets depending on the state of the source: a steady compact jet or a bright transient jet (e.g. Migliari & Fender 2006), depending on the mass accretion rate ($\dot{m}$) and structure of the accretion flow. At lower $\dot{m}$ during the harder X-ray spectral states, the compact jet is characterized by optically thick synchrotron emission exhibiting a flat to inverted radio spectrum ($\alpha \sim 0$, where the radio flux density, S_ν, is proportional to the observing frequency, ν, such that $S_\nu \propto \nu^\alpha$; Blandford & Königl 1979). At higher $\dot{m}$, when the source is softer, the compact jet emission can be quenched (Migliari et al. 2003; Tudose et al. 2009; Miller-Jones et al. 2010; Gusinskaia et al. 2017) and a transient jet is launched, although jet quenching is sometimes not observed (Rutledge et al. 1998; Kuulkers et al. 2003; Migliari et al. 2004; Migliari 2011). Recent results from BH LMXBs suggest that jet quenching at radio frequencies results as the jet spectral break, which is the break from optically thick to optically thin synchrotron emission for the highest energy synchrotron spectra, evolves below the radio band (e.g. Russell et al. 2020), implying that the jet acceleration region shifted away from the compact object (e.g. Markoff, Falcke & Fender 2001; Markoff, Nowak & Wilms 2005). A similar evolution of the jet spectral break is thought to occur in NS systems (Díaz Trigo et al. 2018).

★ E-mail: t.d.russell@uva.nl

Around this time, the short-lived rapidly flaring transient jet can be launched, exhibiting a steep radio spectrum ($\alpha \sim -0.7$) originating from ejected discrete (optically thin) synchrotron emitting plasma (e.g. Fender 2006). Later, as the accretion rate reduces the source transitions back to the hard state and the compact jet re-establishes.

4U 1820−30 is an ultracompact NS LMXB located in the globular cluster NGC 6624, at ≈ 7.6 kpc (Kuulkers et al. 2003). This persistently X-ray bright object displays an ~ 170 d accretion cycle (e.g. Priedhorsky & Terrell 1984; Chou & Grindlay 2001), where the X-ray luminosity evolves between $L_{low} \sim 8 \times 10^{36}(D/7.6\,\mathrm{kpc})^2\,\mathrm{erg\,s}^{-1}$ and $L_{high} \sim 6 \times 10^{37}(D/7.6\,\mathrm{kpc})^2\,\mathrm{erg\,s}^{-1}$ (3–10 keV) (e.g. Priedhorsky & Terrell 1984; Šimon 2003; Wen et al. 2006), which we refer to as low and high X-ray modes, respectively. Generally, in a soft X-ray state, 4U 1820−30 can sometimes transition to a hard state at its lowest mass accretion rates (during low modes; e.g. Tarana et al. 2007; Titarchuk, Seifina & Frontera 2013).

Here, we present broad-band radio observations of 4U 1820−30 taken during its high and low X-ray modes. Observations and analysis are given in Section 2. Section 3 reports the results from the radio observations and connecting the observed changes to the accretion flow. Conclusions are in Section 4.

2 OBSERVATIONS

2.1 Radio

All radio results are given in table 1 of the online supplementary information.

2.1.1 Very Large Array

In total, we present eight radio observations of 4U 1820−30 from the Karl G. Jansky Very Large Array (VLA). The VLA observed 4U 1820−30 on 2018 December 9 (MJD 58461; project code 18A-194) and 2020 July 7 (MJD 59037; project code 20A-255), with data taken at *L* band (1–2 GHz), *C* band (4.5–5.5 and 7–8 GHz), and *K* band (18–19 and 25–26 GHz), where all bands were observed within a 2 h window but not simultaneously. For these radio observations, 3C 286 was used for bandpass and flux calibration, and J1820−2528 was used for phase calibration. The VLA also observed NGC 6624 five times between 2018 May 22 and 28 (MJDs 58260, 58261, 58262, 58265, and 58266) under project code 18A-081 (Shishkovsky et al. 2020). Those data were recorded at the *X* band (8–12 GHz), with durations of 1 or 2 h. Flux and bandpass calibration were done using either 3C 286 or 3C 48 and phase calibration used J1820−2528. Due to flaring of 3C 48 at the time of these VLA observations, a 10 per cent uncertainty was added in quadrature to the measured errors for those epochs.

Using the Common Astronomy Software Application (CASA version 5.1.2; McMullin et al. 2007), data were edited for radio frequency interference and systematics, before being calibrated following standard procedures. *L*- and *C*-band observations were imaged with a Briggs robust parameter of 0 to balance sensitivity and resolution. *K*- and *X*-band data were imaged with natural weighting to maximize sensitivity. To characterize the radio spectral behaviour, the *L*- and *C*-band observations were separated into 4×256 and 4×512 MHz sub-bands, respectively. The *X*-band observations were separated into 4×1 GHz sub-bands. The radio flux density of the target was determined by fitting for a point source in the image plane using a Gaussian with a full width at half-maximum set to the synthesized beam of the observation.

2.1.2 Australia Telescope Compact Array

The Australia Telescope Compact Array (ATCA) observed NGC 6624 on 2006 July 5 (MJD 53921), 2006 July 23 (MJD 53939), and 2006 August 8 (MJD 53955) under project code C1559. These observations were recorded simultaneously at 4.80 and 8.64 GHz, with a bandwidth of 104 MHz at each central frequency. ATCA also observed the target field on 2015 April 24 (MJD 57136) and 2015 April 25 (MJD 57137) under project code C2877 (see Tremou et al. 2018; Tudor et al., in preparation). These two later observations were carried out at central frequencies of 5.5 and 9 GHz, and recorded using the Compact Array Broad-band Backend (Wilson et al. 2011), providing an increased bandwidth of 2 GHz at each central frequency. All ATCA observations used PKS 1934−638 for primary calibration and 1822−36 for phase calibration. Data were edited, calibrated, and imaged (using a natural weighting) as described earlier.

2.2 X-ray

2.2.1 Monitor of All-sky X-ray Image, Swift Burst Alert Telescope, and RXTE All-Sky Monitor

Daily count rates in the 2–20 keV band were obtained from the *Monitor of All-sky X-ray Image* (*MAXI*) X-ray telescope (Matsuoka et al. 2009) website.[1] To estimate the X-ray flux at the time of the radio observations, we downloaded the X-ray spectral and rmf files from the *MAXI* website. The data were then analysed using XSPEC (version 12.8; Arnaud 1996) from the HEASOFT software package (version 6.21). Wilms, Allen & McCray (2000) and Verner et al. (1996) were used to account for line-of-sight abundances and photoionization cross-sections. The 2–20 keV X-ray spectra were modelled with an absorbed power law (tbabs × powerlaw) within XSPEC. The N_H was fixed to $3 \times 10^{21}\,\mathrm{cm}^{-2}$ (Bloser et al. 2000). The photon index was left free, resulting in best fits of ≈ 2 for all epochs (in agreement with results presented by Titarchuk et al. 2013). While more complex models are required to understand the accretion geometry of NS LMXBs, the low sensitivity of the *MAXI* data and small changes in the X-ray spectrum over this energy range meant that the data are reasonably well fitted by a simple absorbed power law ($\chi^2 = 734$ with 685 degrees of freedom), such that they provided reasonable estimates on the 2–20 keV flux. More complex models provided similar fluxes.

Swift Burst Alert Telescope (*Swift*-BAT) Hard X-ray Transient Monitor (Krimm et al. 2013) daily count rates (15–50 keV) were obtained from the *Swift*-BAT website.[2]

X-ray count rates from 2006 could not be obtained from *MAXI* as it was not yet employed. For these times, the *RXTE* All-Sky Monitor (*RXTE*-ASM) 2–12 keV light curve was extracted from the ASM Light Curves web page.[3]

3 RESULTS AND DISCUSSION

4U 1820−30 cycles between its high and low X-ray modes every ~ 170 d (e.g. Priedhorsky & Terrell 1984; Šimon 2003). The changes in the X-ray brightness are a consequence of an evolving mass accretion rate and accretion flow structure (Wijnands, Homan & van der Klis 1999; Cornelisse et al. 2003; Zdziarski et al. 2007). This source is also a known radio emitter (e.g. Fruchter & Goss 2000;

[1]http://maxi.riken.jp/top/index.html
[2]https://swift.gsfc.nasa.gov/results/transients/
[3]http://xte.mit.edu/ASM_lc.html

Migliari et al. 2004; Díaz Trigo et al. 2017). In this work, we report on radio observations of 4U 1820−30 taken during both its high and low X-ray modes, showing a dramatic change in the observed jet emission.

3.1 X-ray modes and origin of the radio emission

To determine the X-ray mode of 4U 1820−30 at the time of the radio observations, we inspected *MAXI*, *Swift*-BAT, and *RXTE*-ASM light curves, which clearly show the X-ray modulations (for example, see fig. 3 in the online information). In almost all cases, the *MAXI* data were used to determine the X-ray mode, where the mid-line between the maxima and minima of the periodic light curve occurs at a 2–20 keV *MAXI* count rate of ≈ 1 photons cm^{-2} s^{-1}. For the three 2006 ATCA observations, the X-ray mode was estimated from count rates reported by Titarchuk et al. (2013).

Due to contamination from the nearby pulsar PSR 4U1820−30A (≈ 0.22 arcsec away; Perera et al. 2017), we first explored the broad-band 1–25 GHz radio emission from the source position with multifrequency VLA observations. Like Migliari et al. (2004), we find that the emission below 4 GHz is dominated by the nearby steep-spectrum ($\alpha \sim -2$) radio pulsar, while higher radio frequencies show the flatter spectrum radio emission from 4U 1820−30 (see online information, fig. 4). Hereafter, we only discuss higher frequency ($\gtrsim 4$ GHz) radio emission associated with 4U 1820−30.

3.2 An evolving radio jet between the high and low modes

Our broad-band 4–26 GHz VLA observations of 4U 1820−30 taken in 2018 during a low X-ray mode show a relatively flat radio spectrum ($\alpha = -0.25 \pm 0.18$; Fig. 1), consistent with optically thick synchrotron emission from a self-absorbed compact jet. During the 2020 high X-ray mode, the radio spectrum was steeper ($\alpha = -1.0 \pm 0.4$) and we did not detect radio emission at 22 GHz. This steep radio spectrum is consistent with optically thin synchrotron emission, indicating that the compact jet had switched off at these higher X-ray luminosities. The observed radio emission originated either from a quenched compact jet (where we are now seeing the optically thin synchrotron emission) or from discrete jet ejecta in a transient radio jet (e.g. Fomalont, Geldzahler & Bradshaw 2001; Fender et al. 2004; Migliari & Fender 2006). To determine if the jet changes are consistent for all high and low X-ray modes, we analysed archival VLA and ATCA radio observations (Fig. 1).

3.2.1 Low X-ray modes

In addition to our 2018 VLA observation, there were four additional ATCA radio observations taken during low X-ray modes (two in 2006 and two in 2015). 4U 1820−30 was detected in both 2015 observations and one 2006 observation, exhibiting a relatively flat radio spectrum with radio spectral indices of $\alpha \sim -0.15$, consistent with a compact radio jet.

The 2015 ATCA observations of 4U 1820−30 were taken during a relatively hard X-ray spectral state, i.e. towards the typical island state (IS) of atoll sources (see Fig. 2). These are the first reported radio detections from this source outside of the full soft state (as described by Titarchuk et al. 2013). Interestingly, while the jet emission may have been marginally brighter (by a factor of ~ 1.5–2) at this time (see also Tremou et al. 2018), the radio spectrum ($\alpha \approx -0.15$) was consistent with other low X-ray mode radio observations. Further simultaneous radio and X-ray (spectral and timing) data are needed to accurately identify the X-ray state and to compare the radio emission.

For the two low-mode ATCA observations taken in 2006, the observations occurred prior to the ATCA bandwidth upgrade (Wilson et al. 2011), meaning that the sensitivity was poor and 4U 1820−30 was only detected in one frequency band (detected at 8.64 GHz but not at 4.8 GHz) on 2006 July 23, and not at all on 2006 August 8 (Fig. 1). Using the 4.8 GHz upper limit and 8.64 GHz detection implied a flat spectral index on 2006 July 23, where $\alpha > -0.1$.

3.2.2 High X-ray modes

For the high X-ray modes, we analysed an additional six VLA observations and two ATCA observations. In all cases where good constraints could be placed on the radio spectrum, the spectrum was steep such that $\alpha \sim -1$.

The six VLA observations were taken over 6 d in 2018, following an X-ray maximum as the X-ray brightness decreased. For all of these six VLA observations, faint radio emission was detected from 4U 1820−30 (Fig. 1). Unfortunately, the faintness of these detections meant that we were not able to identify any progressive changes to the radio emission (should they exist) between epochs as the source evolved towards a low X-ray mode. While the measured radio spectrum of each individual epoch could have been consistent with approximately flat stacking, these six observations together provided much tighter constraints on the spectral index, where $\alpha = -1.25 \pm 0.45$, inconsistent (at $\approx 2.9\sigma$) with a flat radio spectrum.

ATCA also observed 4U 1820−30 during a high X-ray mode in 2006. Unfortunately, due to the low sensitivity of those radio observations we were unable to rule out a flat radio spectrum ($\alpha = -0.6 \pm 0.8$).

In addition, Díaz Trigo et al. (2017) reported on 5.5/9 GHz ATCA and 302 GHz Atacama Large Millimeter/submillimeter Array (ALMA) observations from 2014, where the ALMA observations were taken 10 d prior to the ATCA observations. Those observations produced puzzling results, where 4U 1820−30 was detected at 5.5 and 302 GHz, but not at 9 GHz (despite the 5.5 and 302 GHz results indicating that the source should have been detected at 9 GHz). The 9 GHz non-detection was attributed to either atmospheric or systematic effects, or even an additional previously unknown bright millimetre (mm) source close to the position of 4U 1820−30 (to account for the bright 302 GHz emission). However, analysing the *MAXI* X-ray light curves at the time of the ATCA and ALMA observations revealed that, despite occurring only 10 d apart, the two jet observations occurred within different X-ray modes, where the ALMA observations were taken in a low mode and the ATCA observations were taken in a high mode (corresponding to points 11 and 7, respectively, in Fig. 2). Therefore, our results imply that the 9 GHz non-detection was a result of a steep radio spectrum at the time of the ATCA observations (using the 236 μJy per beam 5.5 GHz radio detection and assuming an $\alpha = -0.7$ radio spectrum, 4U 1820−30 should have been ~ 167 μJy per beam at 9 GHz, below the 200 μJy per beam upper limit reported). The standalone ALMA data from Díaz Trigo et al. (2017) suggested a flat/inverted mm spectrum ($\alpha = 1.7 \pm 1.5$) with no strong intra-observational fading or brightening, implying emission from a compact jet. Comparing typical radio flux densities of 4U 1820−30 with the bright (400 μJy) ALMA detection suggests a radio-to-mm spectral index of ≥ 0.15 (as noted by Tremou et al. 2018).

3.3 Quenching of the compact jet emission

Radio observations of 4U 1820−30 have shown a dramatic change in the jet emission between the source's high and low X-ray modes.
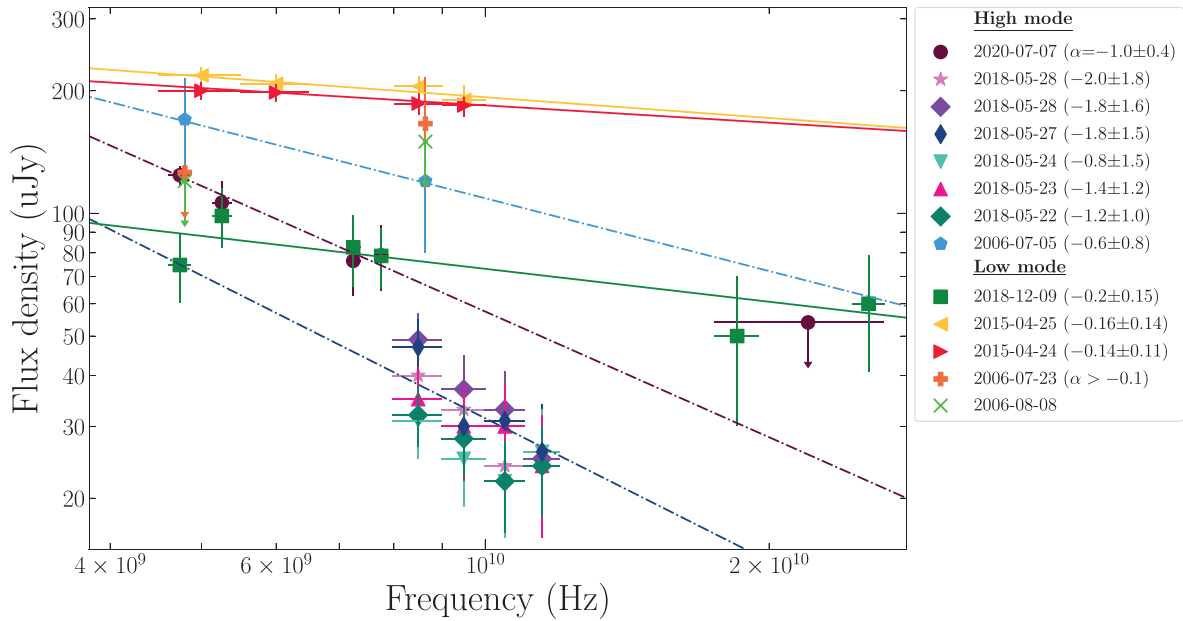
Figure 1. Radio emission from 4U 1820−30 during its high and low X-ray modes. All data are provided in the online information. Fits to each epoch are shown, where dash–dotted lines were used for radio observations taken during high X-ray modes and solid lines were used for low X-ray modes. Radio spectral indices (α) for each epoch are provided in the legend. Due to the radio results showing little difference for the 2018 high-mode data, for clarity, we only show the fit to these observations stacked together (which gives $\alpha = -1.32 \pm 0.54$). Non-detections are shown as 3σ upper limits (determined as three times the image noise). For all observations, when the source was in a high X-ray mode the radio spectrum appeared steep ($\alpha \approx -1$), while during low X-ray modes the radio spectrum was flat ($\alpha \approx -0.15$), indicating a dramatic change in the jet between the X-ray modes.
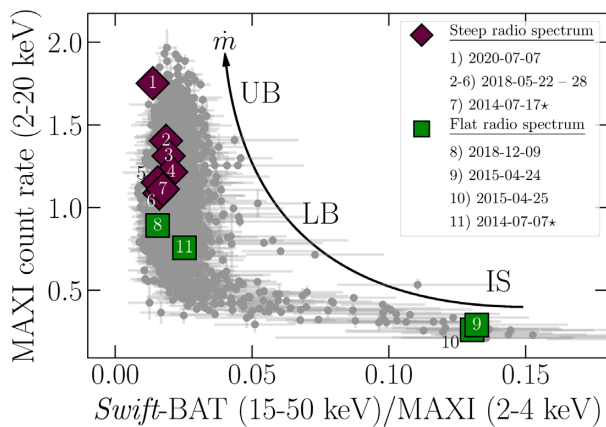
Figure 2. Hardness intensity diagram of 4U 1820−30 (grey markers), indicating the timing of radio observations. Magenta diamonds show radio observations with a steep radio spectrum, while the green squares represent a flat radio spectrum. The approximate locations of the IS, lower banana (LB), and upper banana (UB) spectral branches are displayed (as depicted by Titarchuk et al. 2013), as well as the evolution of the mass accretion rate $\dot{m}$. The numbers correspond to each observational epoch (see the legend). We include the ATCA (high mode) and ALMA (low mode) observations from Díaz Trigo et al. (2017), marked with a ★. The 2006 ATCA detections are not shown due to *MAXI* not being available, but support the conclusions here.

These radio observations indicate that 4U 1820−30 launches a steady compact jet during its low X-ray modes but not during its high X-ray modes (Fig. 1), indicating that the jet is quenched at those times. We also constrain the time-scale of the jet quenching to be less than 10 d. For NS LMXBs, recent results have shown compact jet quenching occurring in less than 2 d (Díaz Trigo et al. 2018), with even shorter constraints for BH systems (Russell et al. 2020). No bright radio flaring was observed, where the observed 5 GHz radio flux densities only varied by a factor of ~2 for all observations. Therefore, while we currently favour a scenario where the high-mode steep-spectrum radio emission arises from the quenched compact jet (following the jet break evolving below the radio band as the jet's first acceleration zone moves away from the compact object; e.g. Russell et al. 2014), further high-cadence radio observations (or sensitive high-resolution very long baseline interferometric radio observations) around the transition are required to identify whether this, or a transient jet, is responsible for the observed radio emission. At present, the shortest time-scale we can place on the launching, flaring, and fading of any transient jet ejecta is ≤10 d (see Section 3.2.2).

3.3.1 Connection to the accretion flow

In BH transients, compact jet quenching is typically associated with a transition from the hard to soft X-ray spectral state. In NS LMXBs, in particular in atoll-type sources, the jet quenching scenario is not so clear, with the jet quenching observed in some sources, but not others (e.g. Migliari 2011; Gusinskaia et al. 2017, for further discussion). In 4U 1820−30, we have observed compact jet quenching that appears to be strongly connected with the accretion rate, where the jet emission transformed at an X-ray flux of ~5.1×10^{-9} erg s^{-1} cm^{-2} (3–10 keV), corresponding to a transition luminosity of ~$3.5 \times 10^{37}(D/7.6\,\text{kpc})^2$ erg s^{-1} (3–10 keV).

Connecting the observed source evolution with the typical atoll-type spectral branches, we find the following: At its lowest mass accretion rate in 4U 1820−30, the X-ray spectrum is hardest (within the IS; Fig. 2), and then as the average mass accretion rate increases the source initially softens before rising at a constant hardness through the LB branch to the UB branch, with the transition of the jet occurring somewhere around the LB state (Fig. 2). In atoll-type

sources, as the mass accretion rate rises (from the LB to UB branch), the electron temperature of the Comptonizing medium (the boundary layer) remains almost constant while the optical depth increases. A change in the boundary layer, along with a simultaneous decrease of the inner disc radius (e.g. Gierliński & Done 2002) could be responsible for the jet changes.

In comparison, in Z-type NS LMXBs, which only show soft X-ray states (but do show some changes in the X-ray hardness), the NS blackbody temperature increases by a factor of ~ 2 when $\dot{m}$ rises within the normal branch, giving an increase of the radiation pressure. Moreover, transient radio jets are launched during this progression (Migliari & Fender 2006). In a unified model for NS LMXBs, Church, Gibiec & Bałucińska-Church (2014) proposed that in both atoll-type and Z-type sources an increase of the radiation pressure may be responsible for disrupting the inner disc and launching transient jets, implying a connection between the jets and the inner accretion disc.

A possible coupling between the jet emission and the boundary layer is an interesting prospect. Such a connection was discussed in a study of the dwarf nova SS Cyg, where the observed radio emission brightened around the time when material first reached the boundary layer and radio flaring was observed when the optical depth of the boundary layer increased such that it became optically thick to itself (Russell et al. 2016). That study speculated that the boundary layer may provide a vertically extended region required for jet launching, analogous to BH and NS LMXBs, where the white dwarf and NS systems have a boundary layer while BH LMXBs contain a geometrically thick accretion flow (i.e. corona; e.g. Zdziarski & Gierliński 2004).

4 CONCLUSIONS

4U 1820−30 periodically cycles between high and low X-ray accretion modes. Using new and archival radio observations of this system during each of these modes, we report on dramatic changes to the jet emission. In all observations where good constraints could be placed on the radio spectrum, 4U 1820−30 launched a flat-spectrum compact jet during its low X-ray modes, which was quenched during the high X-ray modes. In the latter case, the radio spectrum was consistent with optically thin synchrotron emission from either a quenched compact jet where the jet break had evolved below the radio band jet or possibly a transient jet. The changes in the jet appear to be strongly linked to the X-ray luminosity, and hence the mass accretion rate, suggesting a connection to the composition of the inner accretion flow or boundary layer and not the X-ray spectral state. The observations reported here suggest that the radio emission transforms rapidly at an X-ray luminosity of $L_{\mathrm{X}(3-10\,\mathrm{keV})} \sim 3.5 \times 10^{37} (D/7.6\,\mathrm{kpc})^2\,\mathrm{erg\,s^{-1}}$. High-cadence radio and X-ray observations around and after the transition are required to determine precisely when the jet transition occurs, discriminate between the quenched compact jet and transient jet scenario, and identify the specific changes in the accretion flow that may be driving the jet evolution. In particular, X-ray monitoring that includes spectral and X-ray timing information is necessary.

DATA AVAILABILITY

All radio results are provided online. The VLA, ATCA, and ALMA data can be accessed from their online archives. *MAXI*, *Swift*-BAT, and *RXTE*-ASM light curves are publicly available.

REFERENCES

Arnaud K. A., 1996, in Jacoby G. H., Barnes J., eds, ASP Conf. Ser. Vol. 101, Astronomical Data Analysis Software and Systems V. Astron. Soc. Pac., San Francisco, p. 17

Blandford R. D., Königl A., 1979, ApJ, 232, 34

Bloser P. F., Grindlay J. E., Kaaret P., Zhang W., Smale A. P., Barret D., 2000, ApJ, 542, 1000

Chou Y., Grindlay J. E., 2001, ApJ, 563, 934

Church M. J., Gibiec A., Bałucińska-Church M., 2014, MNRAS, 438, 2784

Cornelisse R. et al., 2003, A&A, 405, 1033

Díaz Trigo M., Migliari S., Miller-Jones J. C. A., Rahoui F., Russell D. M., Tudor V., 2017, A&A, 600, A8

Díaz Trigo M. et al., 2018, A&A, 616, A23

Fender R., 2006, in Lewin W., Van der Klis M., eds, Jets from X-ray Binaries. Cambridge Univ. Press, Cambridge, p. 381

Fender R., Wu K., Johnston H., Tzioumis T., Jonker P., Spencer R., van der Klis M., 2004, Nature, 427, 222

Fomalont E. B., Geldzahler B. J., Bradshaw C. F., 2001, ApJ, 553, L27

Fruchter A. S., Goss W. M., 2000, ApJ, 536, 865

Gallo E., Degenaar N., van den Eijnden J., 2018, MNRAS, 478, L132

Gierliński M., Done C., 2002, MNRAS, 337, 1373

Gusinskaia N. V. et al., 2017, MNRAS, 470, 1871

Gusinskaia N. V. et al., 2020, MNRAS, 492, 2858

Krimm H. A. et al., 2013, ApJS, 209, 14

Kuulkers E., den Hartog P. R., in't Zand J. J. M., Verbunt F. W. M., Harris W. E., Cocchi M., 2003, A&A, 399, 663

McMullin J. P., Waters B., Schiebel D., Young W., Golap K., 2007, in Shaw R. A., Hill F., Bell D. J., eds, ASP Conf. Ser. Vol. 376, Astronomical Data Analysis Software and Systems XVI. Astron. Soc. Pac., San Francisco, p. 127

Marino A. et al., 2020, MNRAS, 498, 3351

Markoff S., Falcke H., Fender R., 2001, A&A, 372, L25

Markoff S., Nowak M. A., Wilms J., 2005, ApJ, 635, 1203

Matsuoka M. et al., 2009, PASJ, 61, 999

Migliari S., 2011, in Romero G. E., Sunyaev R. A., Belloni T., eds, Jets at All Scales, Vol. 275, 1st edn. Cambridge Univ. Press, Cambridge, p. 233

Migliari S., Fender R. P., 2006, MNRAS, 366, 79

Migliari S., Fender R. P., Rupen M., Jonker P. G., Klein-Wolt M., Hjellming R. M., van der Klis M., 2003, MNRAS, 342, L67

Migliari S., Fender R. P., Rupen M., Wachter S., Jonker P. G., Homan J., van der Klis M., 2004, MNRAS, 351, 186

Miller-Jones J. C. A. et al., 2010, ApJ, 716, L109

Perera B. B. P. et al., 2017, MNRAS, 468, 2114

Priedhorsky W., Terrell J., 1984, ApJ, 284, L17

Russell T. D., Soria R., Miller-Jones J. C. A., Curran P. A., Markoff S., Russell D. M., Sivakoff G. R., 2014, MNRAS, 439, 1390

Russell T. D. et al., 2016, MNRAS, 460, 3720

Russell T. D., Degenaar N., Wijnands R., van den Eijnden J., Gusinskaia N. V., Hessels J. W. T., Miller-Jones J. C. A., 2018, ApJ, 869, L16

Russell T. D. et al., 2020, MNRAS, 498, 5772

Rutledge R., Moore C., Fox D., Lewin W., van Paradijs J., 1998, Astron. Telegram, 8, 1

Shishkovsky L. et al., 2020, ApJ, 903, 73

Šimon V., 2003, A&A, 405, 199

Tarana A., Bazzano A., Ubertini P., Zdziarski A. A., 2007, ApJ, 654, 494

Titarchuk L., Seifina E., Frontera F., 2013, ApJ, 767, 160

Tremou E. et al., 2018, ApJ, 862, 16

Tudor V. et al., 2017, MNRAS, 470, 324

Tudose V., Fender R. P., Linares M., Maitra D., van der Klis M., 2009, MNRAS, 400, 2111

Verner D. A., Ferland G. J., Korista K. T., Yakovlev D. G., 1996, ApJ, 465, 487

Wen L., Levine A. M., Corbet R. H. D., Bradt H. V., 2006, ApJS, 163, 372

Wijnands R., Homan J., van der Klis M., 1999, ApJ, 526, L33

Wilms J., Allen A., McCray R., 2000, ApJ, 542, 914

Wilson W. E. et al., 2011, MNRAS, 416, 832

Zdziarski A. A., Gierliński M., 2004, Prog. Theor. Phys. Suppl., 155, 99

Zdziarski A. A., Gierliński M., Wen L., Kostrzewa Z., 2007, MNRAS, 377, 1017

SUPPORTING INFORMATION

Supplementary data are available at *MNRASL* online.

online_information.pdf

Please note: Oxford University Press is not responsible for the content or functionality of any supporting materials supplied by the authors. Any queries (other than missing material) should be directed to the corresponding author for the article.

This paper has been typeset from a TEX/LATEX file prepared by the author.